Fusion Engineering and Design 210 (2025) 114729

Contents lists available at ScienceDirect

Fusion Engineering and Design

journal homepage: www.elsevier.com/locate/fusengdes

Comparative analysis of neutronic features for various specimen payload configurations within the IFMIF-DONES HFTM

I. Álvarez [a,*], M. Anguiano [a], F. Mota [b], R. Hernández [c], F. Moro [d], S. Noce [d], Y. Qiu [e], J. Park [e], F. Arbeiter [e], I. Palermo [b], D. Sosa [b]

[a] Department of Atomic, Molecular and Nuclear Physics, University of Granada, UGR, Granada, Spain
[b] Laboratorio Nacional de Fusión por Confinamiento Magnético, CIEMAT, Madrid, Spain
[c] División de Materiales de Interés energético, CIEMAT, Madrid, Spain
[d] ENEA, Nuclear Department, Frascati, Rome, Italy
[e] Karlsruhe Institute of Technology, KIT, Karlsruhe, Germany

ARTICLE INFO

Keywords:
IFMIF-DONES
Neutronics
Comparative
DEMO
DPA
Gas-production

ABSTRACT

The International Fusion Materials Irradiation Facility- DEMO Oriented NEutron Source (IFMIF-DONES) facility is a neutron irradiation facility specifically designed to obtain data on material irradiation for the construction of DEMO (DEMOstration) fusion power plant. The purpose of this study is to investigate and compare the effects of using different realistic models of specimen distribution during the irradiation campaign in the High Flux Test Module (HFTM) in IFMIF-DONES. Parameters such as neutron fluence rate, primary displacement damage rate and gas production have been calculated for two beam footprint sizes: the standard 20×5 cm^2 and the reduced 10×5 cm^2. The standard deuteron beam energy is 40 MeV with a current of 125 mA, but other energy values such as 25, 30 and 35 MeV have also been considered to evaluate their impact on the irradiation parameters. As the idea is to reproduce the DEMO conditions, some neutron spectra in the first wall of the DCLL, WCLL and HCPB have also been evaluated to gather reference data and compare the environments of DEMO and IFMIF-DONES. The level of packaging of the specimens impacts directly the neutron fluence rate behaviour and the different specimen distribution models give rise to different primary displacement damage rate distributions, demonstrating their versatility to meet specific needs. With respect to the comparison DEMO values, IFMIF-DONES meets the requirements of primary displacement damage rate and gas production at different beam energies. This study emphasises the essential role of sample distribution in improving the accuracy of measurements made at the IFMIF-DONES facility.

1. Introduction

The neutron irradiation conditions characterized by high energy neutrons in the future nuclear fusion power plant DEMO imply still large uncertainties for the evolution of material properties over the reactor lifetime. The mission of the International Fusion Materials Irradiation Facility - DEMO Oriented NEutron Source (IFMIF-DONES) [1–3] is to test materials under nuclear fusion irradiation conditions and doses equivalent to those expected in the future DEMO fusion power plant, ensuring their qualification for use. The High Flux Test Module (HFTM) of IFMIF-DONES will be in charge of holding structural materials samples to be irradiated under the typical nuclear fusion irradiation conditions. This neutron source is produced through stripping reaction $D^+ + {}^{6,7}Li$ by a 40 MeV and 125 mA deuteron beam (7.8×10^{17} s^{-1}) impinging on a thick lithium jet, producing a neutron source of about 6.8×10^{16} neutrons/s [4] with a broad spectrum up to 55 MeV and maximum population around 14 MeV. Besides, an important feature of this facility is that the deuteron beam will impinge with a wide footprint of 20×5 cm^2 to cover a great irradiation volume.

The neutron spectrum and the material irradiated are key inputs to obtain the primary displacement damage rate. So, depending on the irradiated material and the irradiation conditions the primary displacement damage rate will be different. The primary displacement damage rate is calculated in displacement per atom [dpa] and it does not take into account other processes related to the diffusion process on the bulk of materials such as recombination, migration, agglomeration, etc.

* Corresponding author.
E-mail address: iac@ugr.es (I. Álvarez).

https://doi.org/10.1016/j.fusengdes.2024.114729
Received 18 July 2024; Received in revised form 22 October 2024; Accepted 11 November 2024
Available online 19 November 2024

The EUROfusion roadmap establishes an initial DEMO phase, where the damage dose requirements are foreseen with a maximum displacement damage dose of around 20 dpa, for steel components integration testing, and a second DEMO phase with a maximum dose of around 50 dpa [5]. However, it is accepted in the IFMIF-DONES white book that, the damage dose requirements suitable to design nuclear fusion equivalent experiments for structural materials are from 10 up to 30 dpa fpy^{-1} in the HFTM [6]. Considering that fpy is a full power year, 365.25 days per year.

The He and H production by transmutation to the number of point defects ratio is also essential to understanding the effect of the radiation on materials [7]. The generation of H and He significantly influences the diffusion of defects and the evolution of damage tracks, whereas the primary displacement damage dose rate directly determines the extent of primary displacement damage caused by neutron interactions [7]. To design equivalent irradiation experiments, it is essential that the gas production to damage dose ratios would be similar to the nuclear fusion reactors.

In this work, the level of damage in EUROFER97 [8] samples inside the HFTM considering different packaging of the samples has been evaluated, both in terms of displacement damage dose and gas production. So far, in the IFMIF-DONES project, the calculations of irradiation conditions in the HFTM area have been made considering a homogenous model (h.m.) of the HFTM capsules where the EUROFER97 specimens were composed of a mixture material of EUROFER97 steel and sodium [9]. In a previous work [10], we have analized this problem considering realistic EUROFER97 specimens models foreseen inside the each HFTM capsule with a low specimen packaging, but conservative respect to design consideration, named CLC.v1.0 [10]. The acronym CLC stands for Capsule Loading Configuration.

Neutron transport calculations have been performed considering a new specimen model, CLC.v2.0 [11] with higher specimen packaging than the previous CLC.v1.0 model. The materials response functions (primary displacement damage dose rate and gas productions) obtained in the specimens have been compared with the ones obtained for previous models, both the homogeneous and CLC.v1.0 models. The different material response functions were obtained for the main deuteron beam footprints considered in the IFMIF-DONES project and different deuteron beam energies.

Besides, comparing the results obtained in IFMIF-DONES with different DEMO concepts is essential because the main objective of IFMIF-DONES is to reproduce the irradiation conditions of the future DEMO. For this purpose, the results obtained for the different material response functions in the HFTM area have been compared with the ones obtained in the first wall (FW) of different DEMO concepts, the Dual Coolant Lithium Lead (DCLL) [12,13], the Water Cooled Lithium Lead (WCLL) [14,15], Helium Cooled Pebble Bed (HCPB) [16–18].

2. Methodology

2.1. Materials and geometry models

The homogeneous model presented before is defined with 75% of EUROFER97 and 25% of Sodium. The first detailed model CLC.v1.0 considered fill the spare spaces of the specimen stack with a high amount of sodium, 48% [10]. Although this metal is very important to reduce the temperature spread among the specimens, it is important to reduce the volume of sodium in several aspects. Sodium is a hazard material due to its chemical reactions with air and water, moreover, its removal from the specimens after the irradiation is a complex operation and it has a higher coefficient of thermal volumetric expansion than the capsule's steel and therefore contributes to thermal-mechanical stresses. But it is necessary to guarantee a good thermal conductivity and a homogeneous temperature distribution.

For this purpose, in CLC.v2.0 the number of specimens has been maximized up to 3840, 608 specimens more than in CLC.v1.0. In fact,

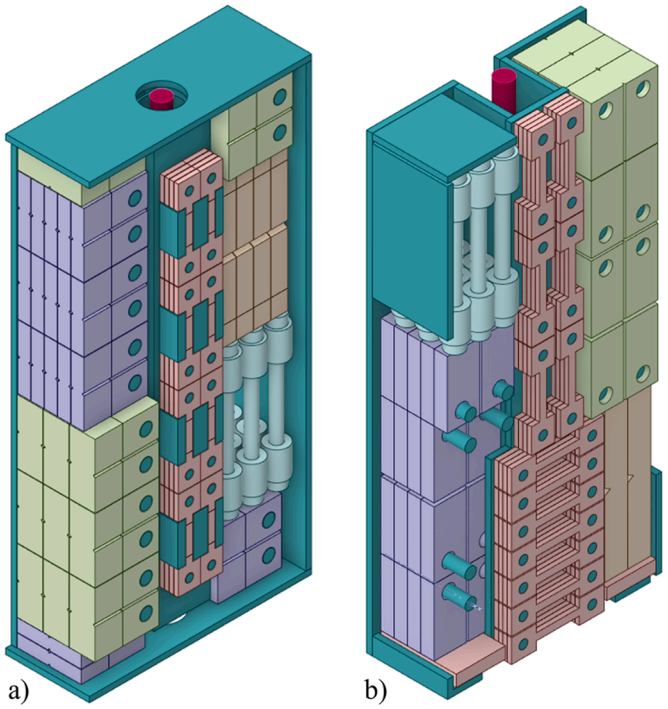

Fig. 1. a) CLC.v2.0 [11] and b) CLC.v1.0 [10] packaging proposal of SSTT in the HFTM specimen stack.

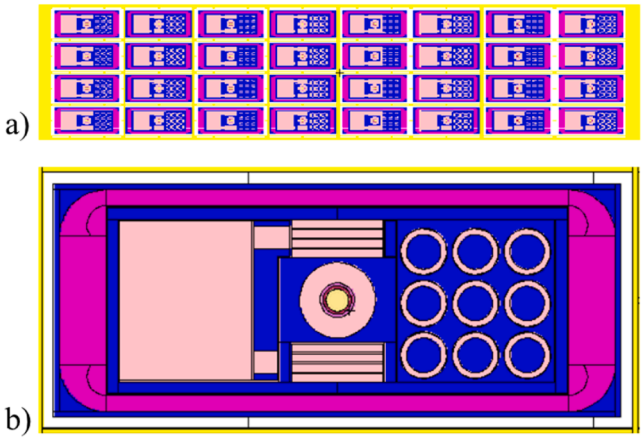

Fig. 2. Horizontal cross-section of the MCNP model of the HFTM with the CLC.v2.0 detailed model of the specimen stacks installed; a) cross-section of the HFTM, b) cross-section of one stack.

block of custom-designed EUROFER97 have been developed to fill specific volumes, thus reducing the percentage of sodium to 12.92%. Additionally, the percentage of EUROFER97 is 84.76%, more similar to the one considered in the homogeneous model. Moreover, those filler pieces can be used for material testing as well. The CLC.v2.0 design is shown in Fig. 1a, and CLC.v1.0 model is in Fig. 1b.

To ensure the maximum number of specimens in the available space, they have been designed with Small Specimen Test Techniques (SSTT). This model contains the same five different types of specimens in CLC.v1.0, following the line of maintaining the minimum number of specimens per type to characterize the damage. The specimen types are 64 flat tensile, 9 cylindrical fatigue, 12 KLST impact, 22 Fatigue Crack Growth (FCG) and 13 Fracture Toughness (FT), a total of 120 specimens per rig. In this case, the hole of the diagnostic has been filled with sodium around diagnostics.

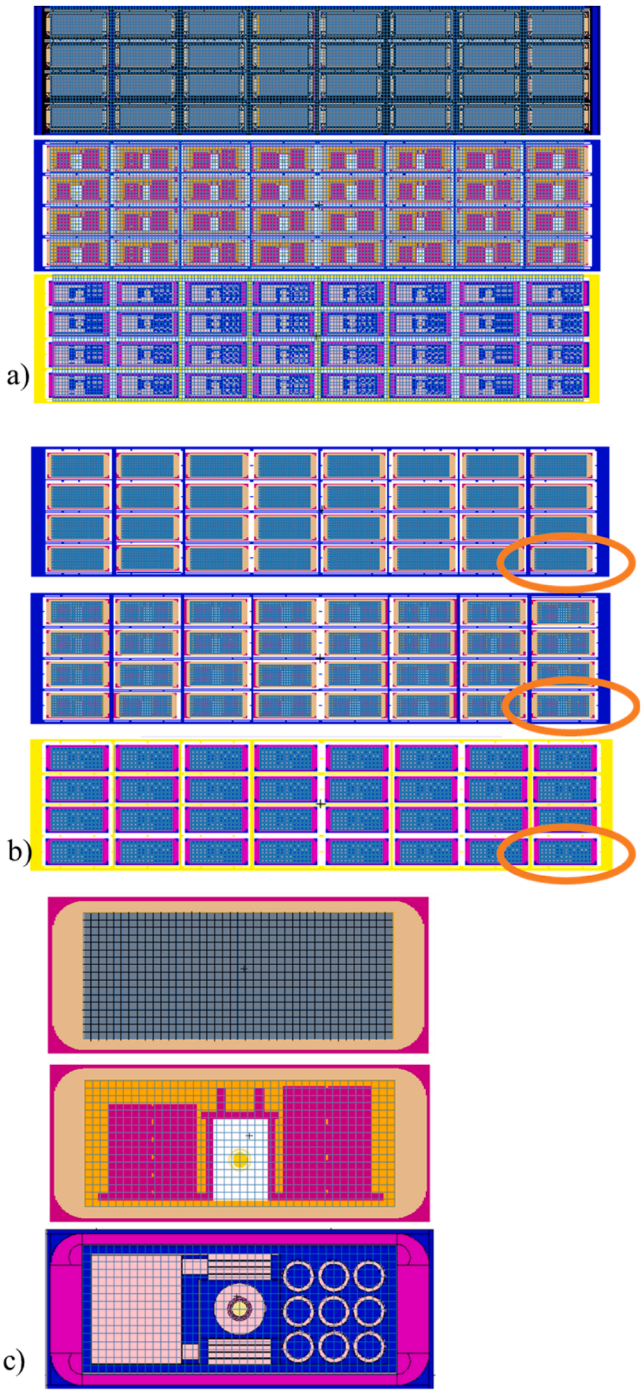

Fig. 3. Horizontal cross section of the HFTM at the middle of the deuteron beam; a) Specimens region mesh for the h.m., CLC.v1.0 and, CLC.v2.0 models. b) Specimens stacks mesh for the h.m., CLC.v1.0 and CLC.v2.0 models. c) Enlargement of the highlighted area in b).

The 3D CAD model of the capsule with the specimens has been simplified using SpaceClaim 2021 R1 software [19]. The main assumptions to make the simplification was to keep the original volume of specimens because it will be important for further activation calculations, which are not presented in this paper. Once the model was simplified, it was converted into the Monte Carlo N-Particles (MCNP6.2) model [20] using TopMC [21] software. A separate model was created for each capsule within the HFTM, and, subsequently, these models were integrated into the overall HFTM model at their respective positions in the updated version of the Test Cell (TC) model "mdl9.2.8". Fig. 2 shows

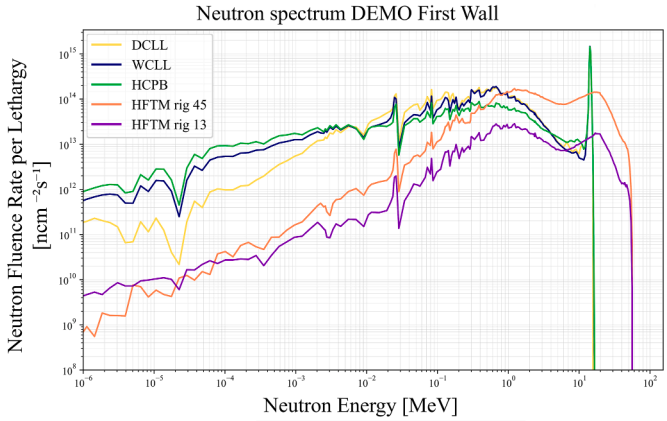

Fig. 4. Neutron spectra of the different DEMO concepts considered, DCLL, WCLL, and HCPB and compared to the neutron spectra obtained in the rigs 13 and 45 inside the HFTM.

a horizontal cross-section of the HFTM in the MCNP model with CLC. v2.0 in each stack (Fig. 2a) and a cross-section of one stack (Fig. 2b).

2.2. Neutron transport calculation methodology

The neutron transport calculations have been performed using McDeLicious code (based on MCNP6.2) developed by the Karlsruhe Institute of Technology (KIT) laboratory to reproduce the IFMIF deuteron–lithium neutron source [22]. Two footprint beam sizes, 10×5 cm^2 and 20×5 cm^2, and beam energies of 25, 30, 35 and 40 MeV have been considered. The FENDL3.1d nuclear data library [23] has been used for neutron transport calculations.

As mentioned in the introduction, the irradiation parameters calculated to assess the radiation effect on EUROFER97 specimens in the HFTM areas include the primary displacement damage rate and He and H production to displacement damage dose ratios. All response functions have been integrated for a full power year [fpy] of 365.25 days per year as commented before.

The primary displacement damage rate has been calculated using both accepted methodologies, the Norgett Robinson Torrens (NRT) [24] and arc_DPA methods [25]. Although the arc_dpa method was developed to improve the way to determine the primary displacement damage, based on the most recent molecular dynamics simulations, it is essential to continue using the NRT model to compare results with older databases of primary displacement damage calculations. To determine the NRT and arc_dpa primary displacement damage, the nuclear data library used has been JEFF3.3DPAarc [26]. The calculation of H and He production has been done integrating the neutron spectrum with gas production cross section MT203 and MT207, respectively, from the FENDL3.1d nuclear data library. The response functions in the irradiated area of the HFTM have been determined using two approaches: first, by applying meshes that cover the entire area of the HFTM capsules, and second, by analyzing each of the individual capsules.

In order to assess better the available space to hold specimens, two different meshes have been used to tally the results. First, one encompassing the whole HFTM area (Fig. 3a), named specimen region (i), and the second one, composed of a set of meshes where each one covers the inner volume of each capsule, in order to exclude the structural parts of the HFTM, named specimen stack mesh (ii) (Fig. 2b). The specimen region mesh (i) has a resolution of $2.5 \times 2.5 \times 2.5$ mm^3, while the specimen stack mesh (ii) $1.0 \times 1.0 \times 1.0$ mm^3.

As mentioned above, the calculated response functions in the HFTM area were compared with the ones obtained in the FW of the different DEMO concepts, that depend on the specific breeding blanket technology used for tritium production. Two liquid breeding blanket types have been considered, DCLL [12,13] and WCLL [14], alongside one solid

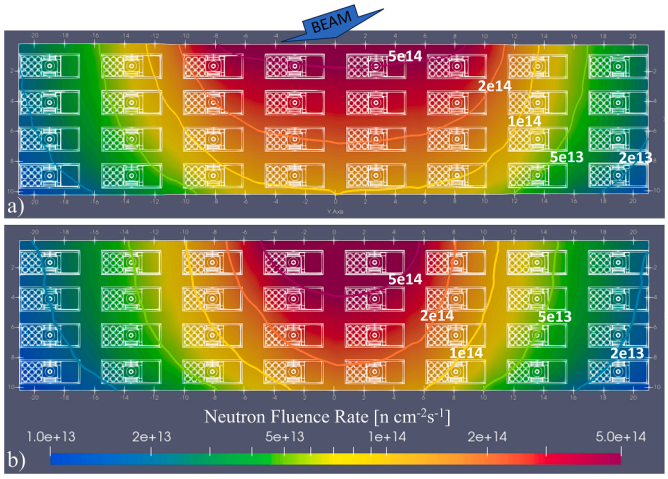

Fig. 5. Horizontal cross section of the Neutron fluence rate maps [ncm^{-2}s^{-1}] of CLC.v2.0 at the middle of the deuteron beam; a) 20×5 cm^2 and b) 10×5 cm^2 footprint size.

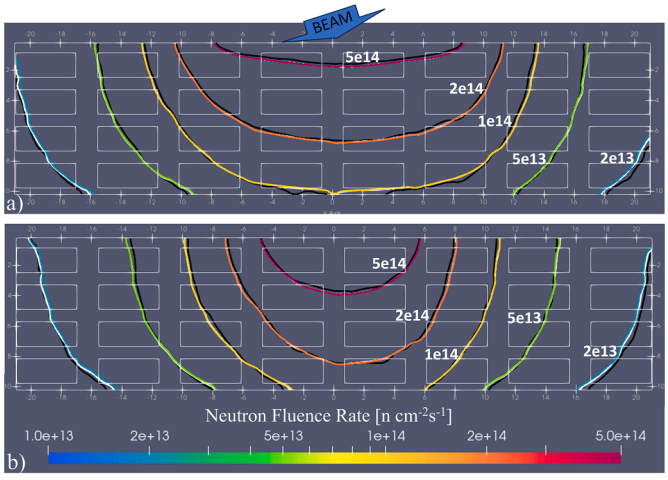

Fig. 6. Horizontal cross section of the neutron fluence rate maps [ncm^{-2}s^{-1}] for three models at the middle of the deuteron beam: white lines-CLC.v2.0, black lines-CLC.v1.0 and colour lines-h.m.; a) 20×5 cm^2 and b) 10×5 cm^2 footprint size.

breeding blanket concept HCPB [16]. In all the cases, the same nuclear fusion power (1998 MW) has been used, with a normalized neutron source of 7.094·10^{20} ns^{-1}. The geometrical models were developed for the different research laboratories in charge of their development, DCLL by CIEMAT [12,13], WCLL by ENEA [14,15] and HCPB by KIT [16,17,18] laboratory. In Fig. 4 the corresponding neutron spectra in the FW are shown along with the neutron spectra range in IFMIF-DONES. The response functions for DEMO are calculated using each neutron spectrum as the neutron source in a simple MCNP geometry, which consists of two concentric spheres. The main assumptions to perform these calculations are the following; first, the neutron source gets out from a spherical surface of 1 cm^2, because the neutron spectrum is given in n·cm^{-2}s^{-1} and second, the response functions are tallied in a spherical shell with thin enough of EUROFER97 so that the attenuation of the neutron spectrum is small. The radius of the first sphere is 0.289 cm and that of the concentric sphere 0.4 cm. Besides, as even so, there will be some neutron attenuation, the response functions are normalized by the attenuation to compensate the losses.

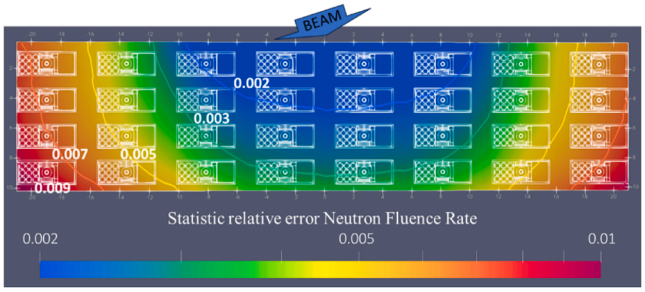

Fig. 7. Horizontal cross-section of the statistic relative error of the neutron fluence rate maps of the CLC.v2.0 model at the middle of the 20×5 cm^2 deuteron beam footprint size.

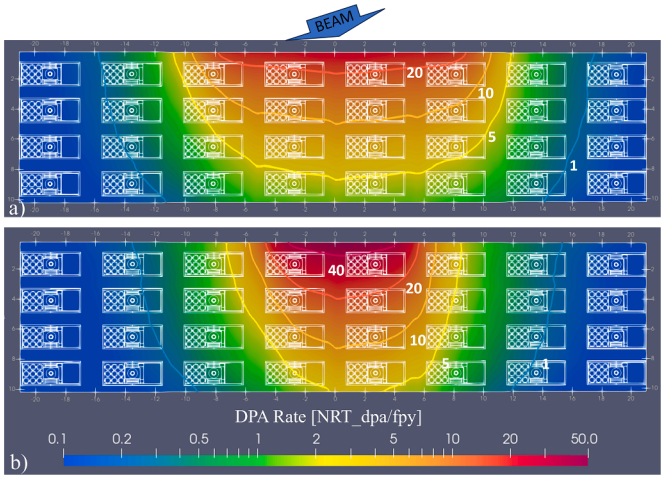

Fig. 8. Horizontal cross-section of the primary displacement damage rate [NRT_dpa/fpy] of the CLC.v2.0 specimen stacks at the middle of the deuteron beam; a) 20×5 cm^2 and b) 10×5 cm^2 footprint size.

3. Results

This section presents a comparative analysis of neutron fluence rates, primary displacement damage rates, and gas production (He and H) to displacement damage dose ratios for the CLC.v2.0 and a comparison with the previous models: the homogeneous and CLC.v1.0 ones. Furthermore, the same results are shown for different beam energies and their comparison with the data calculated for DEMO.

3.1. Neutron fluence rate

A cross-section of the neutron fluence rate map at the midpoint of the deuteron beam is shown in Fig. 5 for the CLC.v2.0 using different footprint sizes. As it happened for the other models, the neutron fluence rate is higher in the two central rigs for the 10×5 cm^2 footprint size, while the 20×5 cm^2 footprint size is extended to the four central rigs.

To understand better the differences of neutron fluence rate using different models in the rigs of the HFTM, Fig. 6 shows the isobar lines for each model. The coloured lines correspond to the homogeneous model, the black lines to the CLC.v1.0 and the whites to the CLC.v2.0. The level of packaging of CLC.v2.0 and homogeneous is very similar, so the lines are very near, while the CLC.v.1.0 has a lower level, their lines have a bit displacement respect the others. With this image, it is also easier to see the differences when the beam size footprint changes. The central rigs are enhanced while the farthest corners decrease easily.

Fig. 7 shows the statistic relative error for the 20×5 cm^2 beam footprint and for the CLC.v2.0. All the uncertainties are between 0.2 and 1%, so they are sufficiently small over the whole area of interest [20].

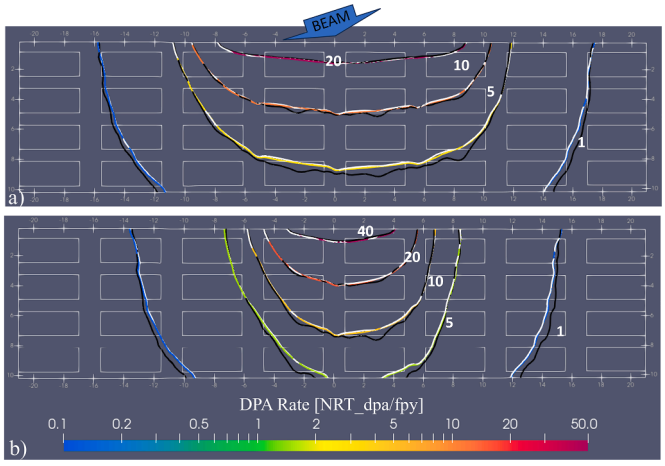

Fig. 9. Horizontal cross the primary displacement damage rate [NRT_dpa/fpy] for three models at the middle of the deuteron beam: white lines-CLC.v2.0, black lines-CLC.v1.0 and colour lines-h.m.; a) 20×5 cm^2 and b) 10×5 cm^2 footprint size.

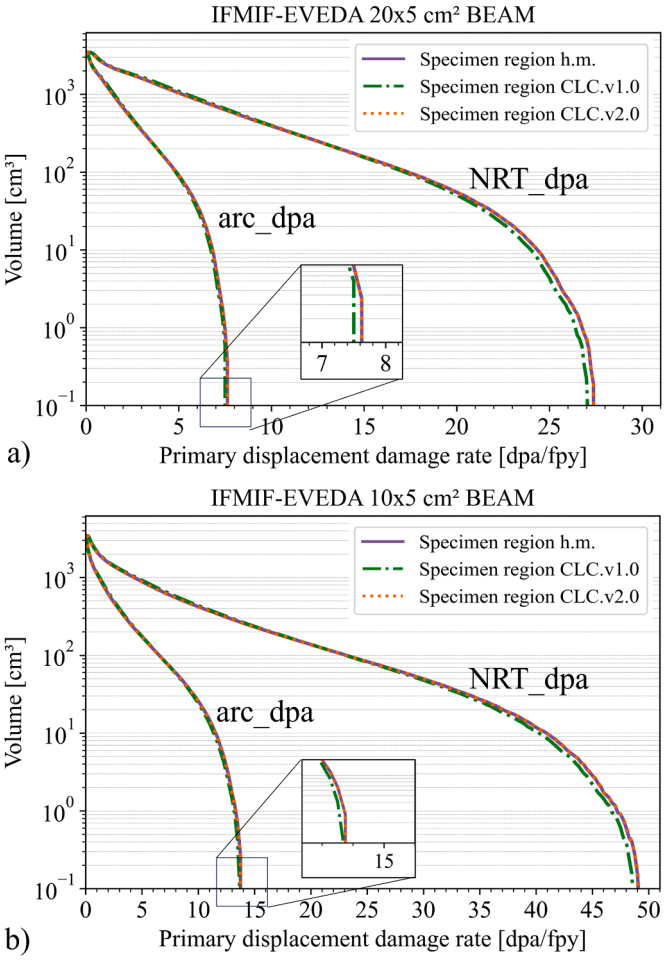

Fig. 10. Available integrated irradiation volume (32 rigs) versus primary damage dose rate [arc_dpa/fpy] and [NRT_dpa/fpy] for the different specimens stacks model in the HFTM volume: h.m., CLC.v1.0 and CLC.v2.0.; a) 20×5 cm^2 and b) 10×5 cm^2 footprint size.

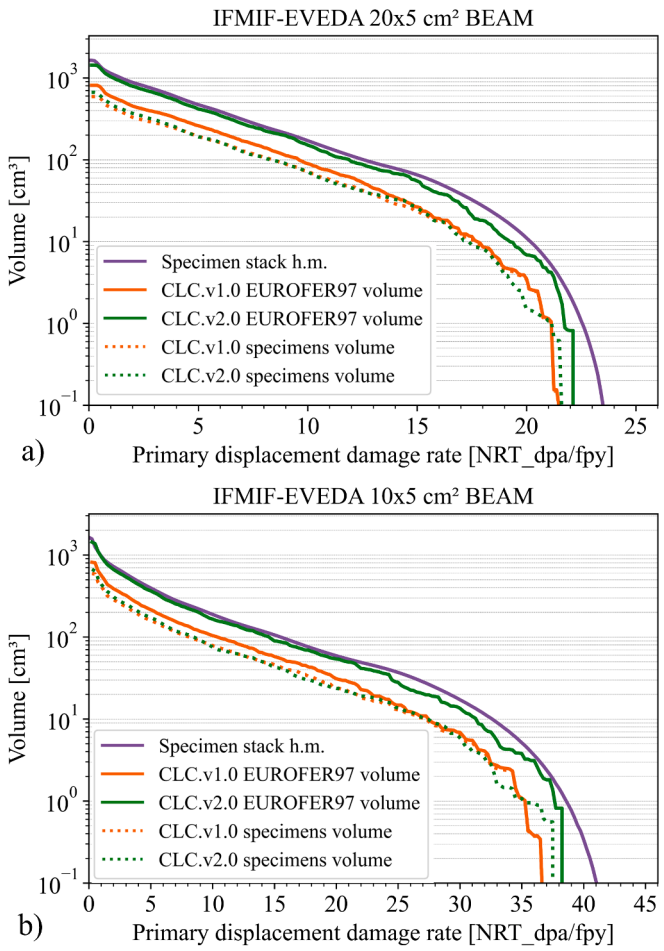

Fig. 11. Available integrated irradiation volume (32 rigs) versus primary damage dose rate [NRT_dpa/fpy] for the different specimens stacks model: Homogeneous, CLC.v1.0 and CLC.v2.0.; a) 20×5 cm^2 and b) 10×5 cm^2 footprint size.

Moreover, it can be observed that in the region where the neutron fluence rate is higher, the uncertainties are lower.

3.2. Primary displacement damage rate

In order to achieve the goals, set for DONES, it is essential that the required primary displacement damage rate is achieved in the HFTM. This rate, expressed as displacement per atom (dpa) per full power year (dpa/fpy), is a critical metric. By integrating the neutron flux with the EUROFER97 dpa production cross section, the primary displacement damage is determined. As mentioned above, this assessment of primary displacement damage has been carried out using both the NRT model and the arc_dpa model methodologies.

Figs. 8 and 9 show the primary displacement damage rate in a horizontal map in the middle of the deuteron beam, for both footprint sizes, 20×5 cm^2 (a) and 10×5 cm^2 (b). In Fig. 8 the distribution of primary displacement damage rate corresponds to the CLC.v2.0 specimen distribution. As for the neutron fluence rate, the highest values are in the four central rigs for the 20×5 cm^2 footprint, while for the reduced one the targeted part are the two central rigs. In Fig. 9 a comparison of the primary displacement damage ratio with the three models is depicted. In the figure, the homogeneous model results are the coloured lines, the CLC.v1.0 ones are the black lines and those corresponding to the CLC.v2.0 model are the white lines. As the level of packaging for the CLC.v2.0 is quite similar to the homogenous model, the NRT_dpa values calculated for both models suit very well.

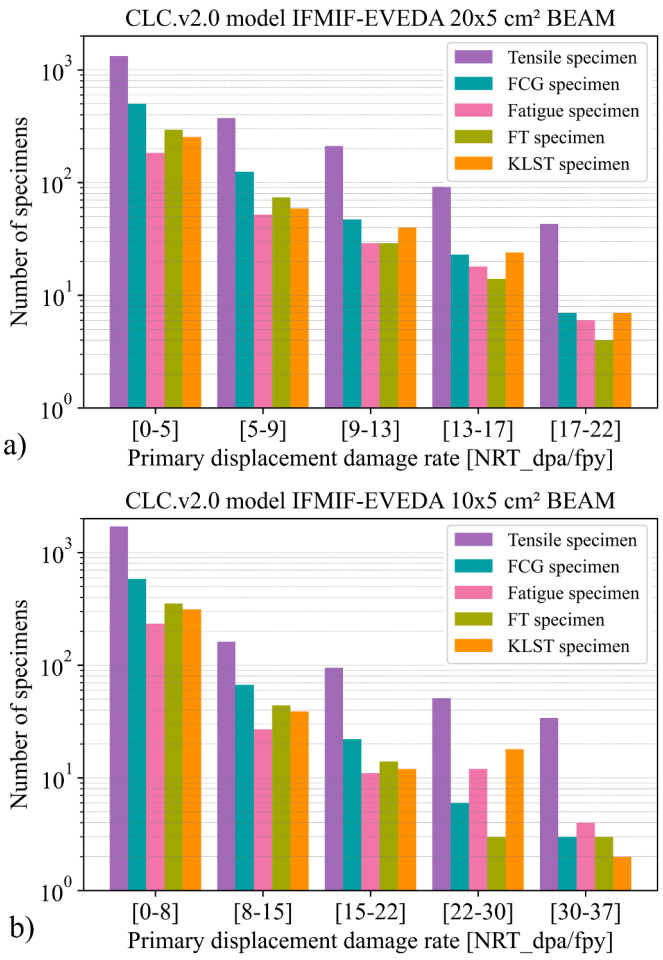

Fig. 12. Histogram of the number of available samples by type versus primary damage dose rate [NRT_dpa/fpy] for the CLC.v2.0 model; a) 20×5 cm^2 and b) 10×5 cm^2 footprint size.

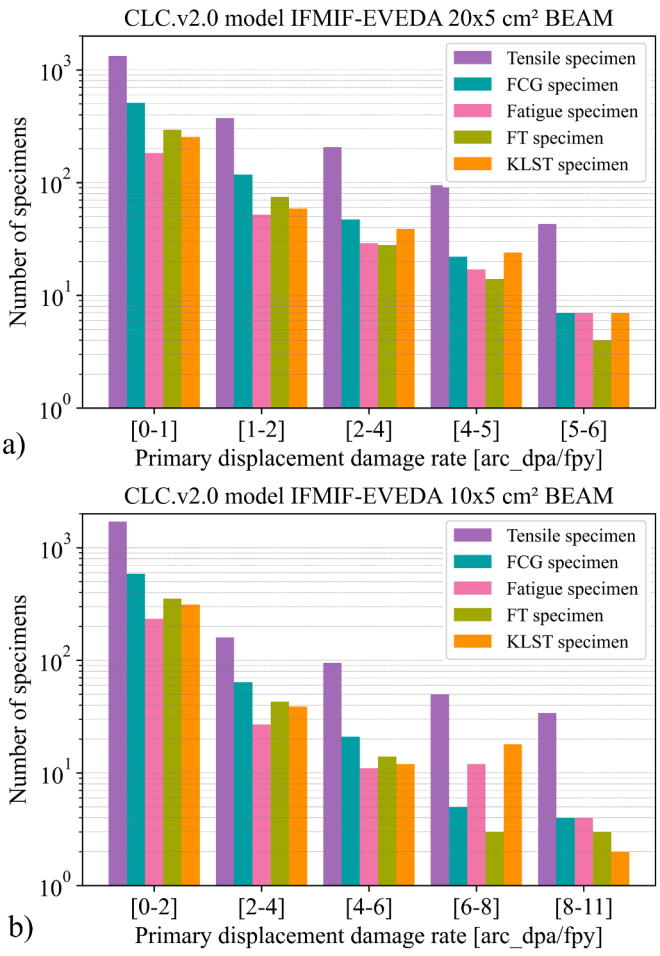

Fig. 13. Histogram of the number of available samples by type versus primary damage dose rate [arc_dpa/fpy] for the CLC.v2.0 model; a) 20×5 cm^2 and b) 10×5 cm^2 footprint size.

The primary displacement damage in arc_dpa/fpy and NRT_dpa/fpy is shown in Fig. 10. The trend shows the same behaviour with both calculation methods, changing the range of values over which they oscillate. For the 20×5 cm^2 beam footprint (Fig. 10a) the arc_dpa/fpy values are between [0–8] and NRT_dpa/fpy values [0–28] and for the 10×5 cm^2 beam (Fig. 10b) the arc_dpa/fpy values are between [0–14] and NRT_dpa/fpy values [0–50]. Generally, the NRT_dpa values are higher than arc_dpa values because this model has not taken into account recombination processes during the thermal spike. In addition, both models for calculating the primary displacement damage rate show similarities in the results when comparing the models. The homogeneous and CLC.v2.0 models fit very well, mainly due to the fact that the level of packing is very similar in both cases as previously commented, with the lines overlapping. This is important conclusion that, the homogenous model assumption used in the past is justified. Another benefit is, using the homogeneous model can reduce computing time by a factor of 1.4 for the same calculations, thus more efficient for simulations e.g. shielding analysis. On the other hand, the values of the CLC.v1.0 model are shifted a little to the left. The primary distinction between different beam size footprints lies in the amount of dpa achieved in each specific case. Using the reduced beam footprint (panel b), the highest value of NRT_dpa can reach around 49 dpa/fpy in low volume, while with the standard beam (panel a) 27 dpa/fpy is reached at the front of HFTM.

When compared to previous calculations in [10], both the values of NRT_dpa and arc_dpa show a slight increase. This is because, in this case, the primary displacement damage has been obtained in the equivalent EUROFER97 displacement damage instead of on the equivalent iron displacement damage.

Fig. 11 shows five different cases. The solid line for the homogeneous model takes into account only the volume in the stack, MESH (ii). For the detailed models, there are two cases. The first, continuous lines, take into account all the EUROFER97 vol (i.e. the specimens volume plus the volume of filling blocks); for this reason, the volume is higher for the two models. The second, dotted lines, consider only the specimens volume. It can be seen in Fig. 11 that the EUROFER97 vol (solid lines) in the CLC.v2.0 model is higher than in the CLC.v1.0 one, and that this volume is practically the same obtained for the homogeneous one. On the other hand, since in the CLC.v1.0 the volume of filling blocks is very low, the highest dpa reached for both cases are the same since the lines overlap. In the case of the CLC.v2.0 model, the solid line reaches a higher value than the specimen case (dotted line). This could be interesting because that means that, in the CLC.v2.0 model, the filling block is placed in front of the specimens and just in the first line of the beam in case of the central rigs. In this way, these pieces are the ones that reach the highest dpa values. Specimens which are behind these filling blocks receive an already moderated neutron flux. If the idea is to improve the dpa data for specimens, it could be interesting to place them in the first line of the beam and put the filling object behind. In addition, rotating the model and comparing the data could be considered.

Fig. 12 indicates a histogram with the number of specimens available in the different ranges of dpa values for the standard beam footprint (a) and the reduced one (b) for the CLC.v2.0 model. This type of plot was shown in [10] for the CLC.v1.0 model. Taking into account both images,

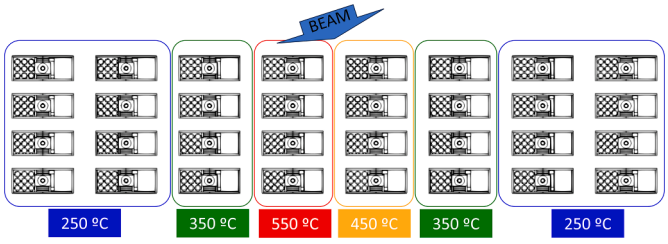

Fig. 14. Temperatures distribution in the HFTM [27].

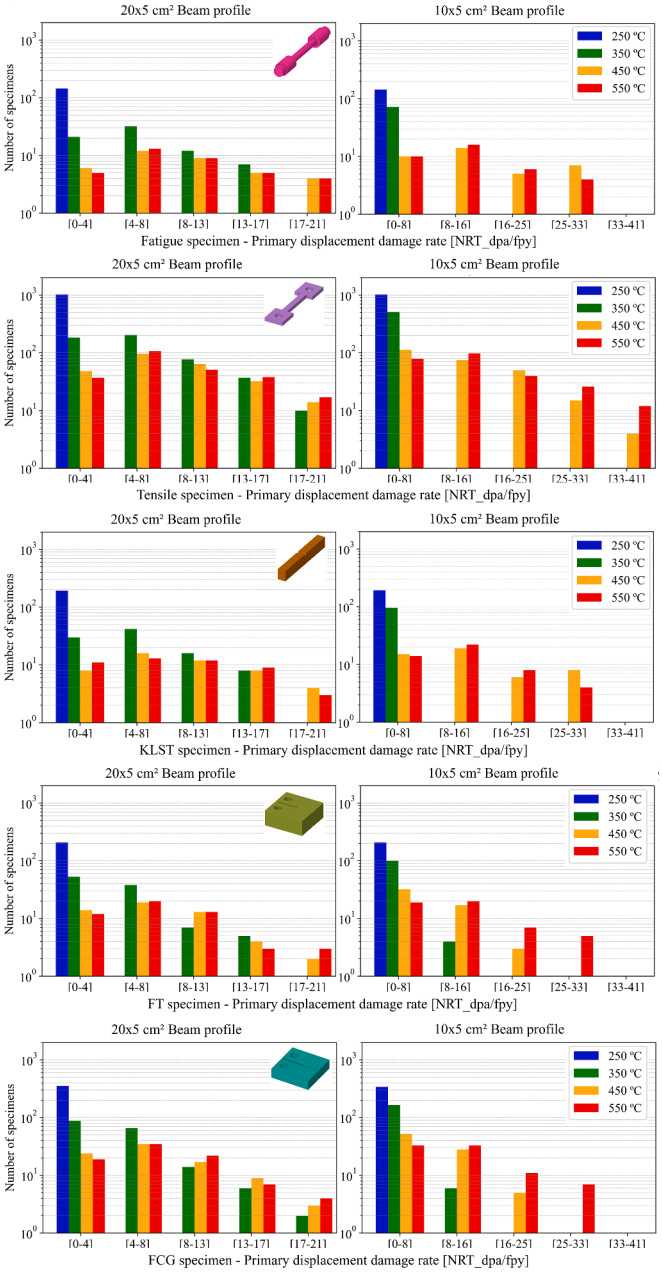

Fig. 15. Histogram of the number of specimens by type and temperature versus primary damage dose rate [NRT_dpa/fpy] for a 20×5 cm ^{2} (left panel) and 10×5 cm^2 footprint size (right panel).

it can be demonstrated that a change in the distribution of specimens inside the stack, can change the number of specimens available depending on the dpa value. With CLC.v2.0 model, there are all

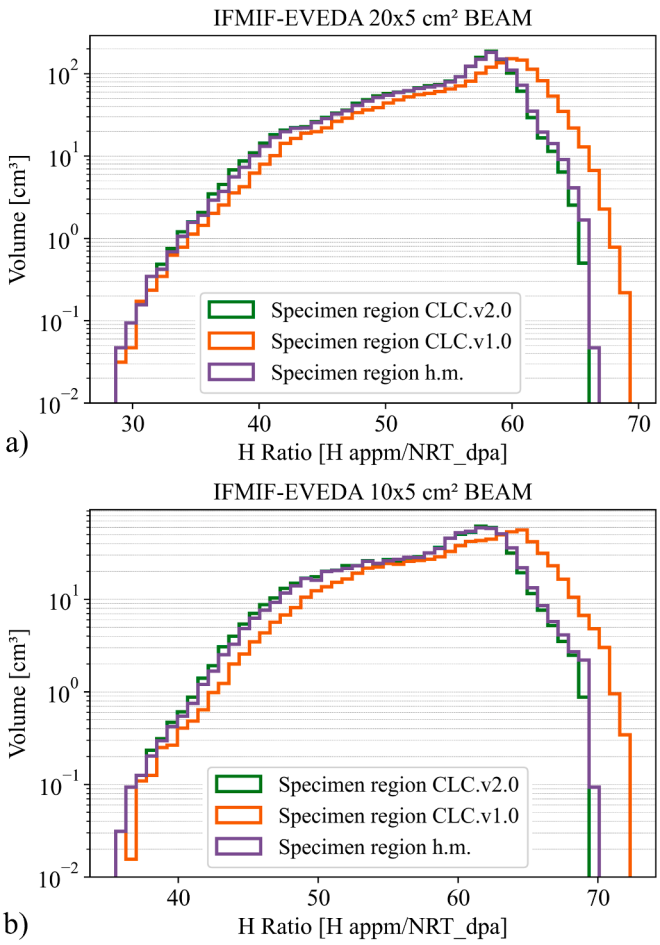

Fig. 16. Irradiation volumes as function of H-NRT_dpa ratio, using a) 20×5 cm^2 and b) 10×5 cm^2 footprint size.

specimen types in all the ranges of dpa, while with CLC.v1.0 some specimen types are subject to the highest range of dpa. Moreover, for the case of CLC.v2.0 shown in Fig. 12, for the reduced beam footprint, panel b), the range of DPA values is wider than the standard beam footprint, panel a), where they are distributed in a small range.

To compare the results of NRT_dpa and arc_dpa, Fig. 13 shows the distribution of the different types of specimens depending on the arc_dpa/fpy value, as in Fig. 12 for the NRT_dpa/fpy. The tendency is practically the same but in a lower range of values. There are all the types of specimens in each range of arc_dpa value for the two beam footprints, as happened with the NRT_dpa.

Based on [27] the temperatures expected in each rig are those shown in Fig. 14, although they can change depending on the needs. The range is from 250 °C to 550 °C and they are defined by slot. The idea is to maintain them constantly throughout the irradiation campaign using heaters and a helium cooling system to remove the nuclear heating. Taking these temperatures as the starting point, the amount of specimen per type and NRT_dpa (the calculations for the arc_dpa values are the same) values available have been calculated and it is shown in Fig. 15 for the 20×5 cm^2 beam footprint size (Fig. 15-left) and for the 10×5 cm^2 one (Fig. 15-right). There are significant changes between the different footprint sizes. In all the cases, the number of specimens at the lowest temperatures is always in the lowest range of dpa values, since those temperatures are in the external slot and then, at the farthest part from the beam. In the case of the standard beam, the other temperature values are more or less distributed between the dpa ranges, and always the lowest number of specimens is the highest range of dpa values. In the case of the reduced beam, as it is more focalized, it reaches higher

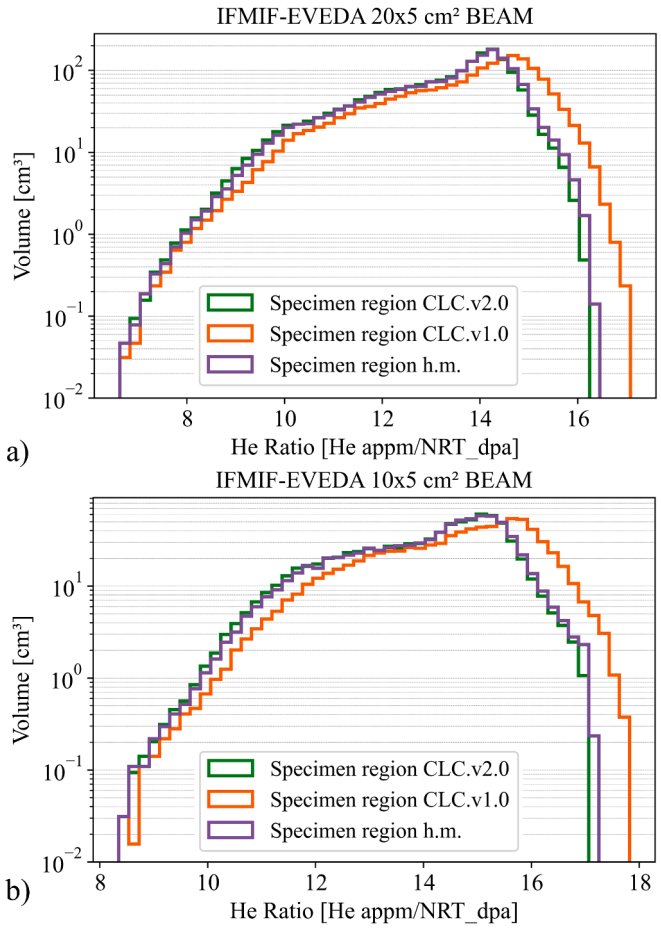

Fig. 17. Irradiation volumes as function of He-NRT_dpa ratio. Using a) 20×5 cm^2 and b) 10×5 cm^2 footprint size.

values, but the distribution is less homogeneous. Furthermore, when breaking down the data it can be seen that not all the specimen types reach the highest values of dpa, only the tensile type has specimens in all the dpa ranges. On the other hand, all FT and FCG specimens at the highest dpa values are at 550 °C. So, the reduced beam generates a heterogeneity concerning the temperature distribution.

3.3. Gas production to displacement damage ratio

This parameter exhibits a synergistic impact with displacement damage evolution, directly shaping the diffusion of displacement defects [7] on materials. The units used in this part for the H/dpa ratio are [H appm/NRT_dpa] and for the He/dpa ratio are [He appm/NRT_dpa]. Only the volume of the 16 central rigs is considered to obtain the gas production for a 20×5 cm^2 and 8 rigs for a 10×5 cm^2. The main difference in the ratios related to the footprint beam size is the maximum peak of volume. In Fig. 16 and Fig. 17 can be observed this tendency. This happens mainly because, for the reduced footprint beam case, the maximum dpa values are reached in the central 8 rigs, while for the standard beam are 16 central rigs, so, the volume increases for lower gas production ratios. The values obtained for the CLC.v2.0 model match better with the results obtained for the homogeneous model than for the CLC.v1.0 model due to the EUROFER97 packing level. This happens for both, H and He ratios. Apart from that, the peak values of 55–60 H-appm/dpa and 14–16 He-appm/dpa are in the range expected for DEMO [28,29]. In the next section, these results are also compared with the data determined from the DEMO spectra shown in Fig. 4.

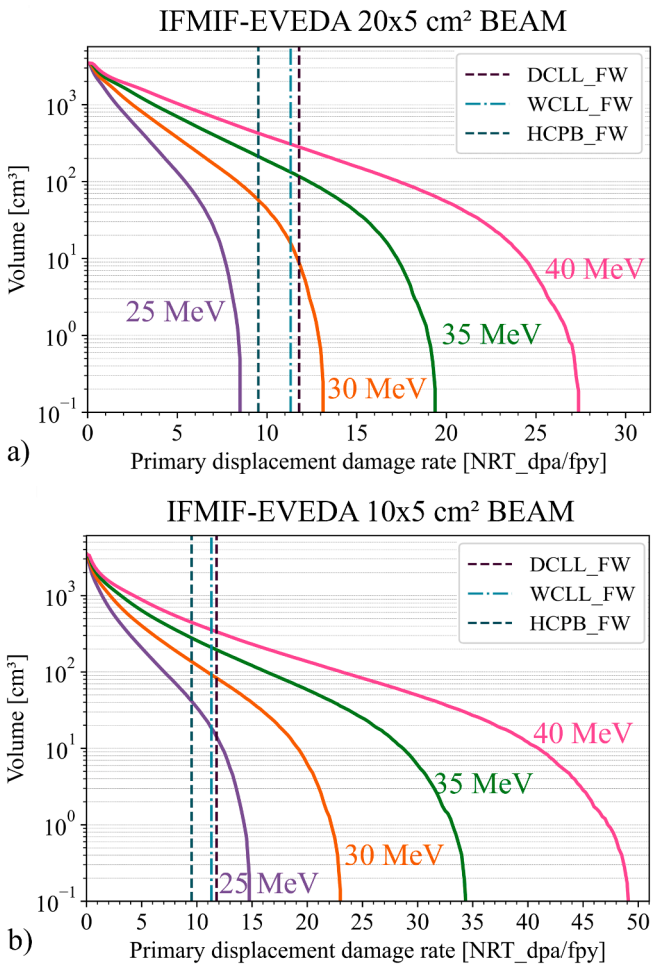

Fig. 18. Available integrated irradiation volume versus primary damage dose rate [NRT_dpa/fpy] for the CLC.v2.0 model for 25, 30, 35, 45 MeV energy beam; a) 20×5 cm^2 and b) 10×5 cm^2 footprint size.

3.4. Primary displacement damage and gas production rates for different beam energies

For the CLC.v2.0 model, the previous data of NRT_dpa and gas production rate has been obtained for the standard energy of the beam, that is 40 MeV, but it is also interesting to test how modifies the previous results changing this energy. In this section, we compare the data for different beam energies of 25, 30, 35 and the standard one, 40 MeV. Moreover, the data obtained in the inboard first wall for DCLL [12,13], WCLL [14,15] and HCPB [16–18] are shown in each figure in order to compare with the different cases.

Fig. 18 shows that as lower the beam energy, the lower the displacement damage rate reached in each case. Vertical lines correspond to the values calculated for each DEMO configuration. All data for DEMO are around 10 NRT_dpa/fpy. The range of NRT_dpa reached with the standard beam (Fig. 18a) is from 8 to 27 NRT_dpa/fpy depending on the beam energy, which means that using the highest energy of 40 MeV in a 1 fpy of IFMIF-DONES can be reproduced almost 3 fpy of DEMO. In the case of the reduced beam foot print of 10 × 5 cm^2 (Fig. 18b) the range of NRT_dpa/fpy reached according to the beam energy is from 15 to 49, so in this scenario, IFMIF-DONES can reproduce more than 1 DEMO fpy with the lowest energy of 25 MeV in just 1 fpy, up to almost 5 DEMO fpy using the higher beam energy.

The case of the arc_dpa calculation is shown in Fig. 19. As presented before, the range of arc_dpa reached is lower than the range of NRT_dpa. Using the spectrum of Fig. 4 to obtain the arc_dpa values for different

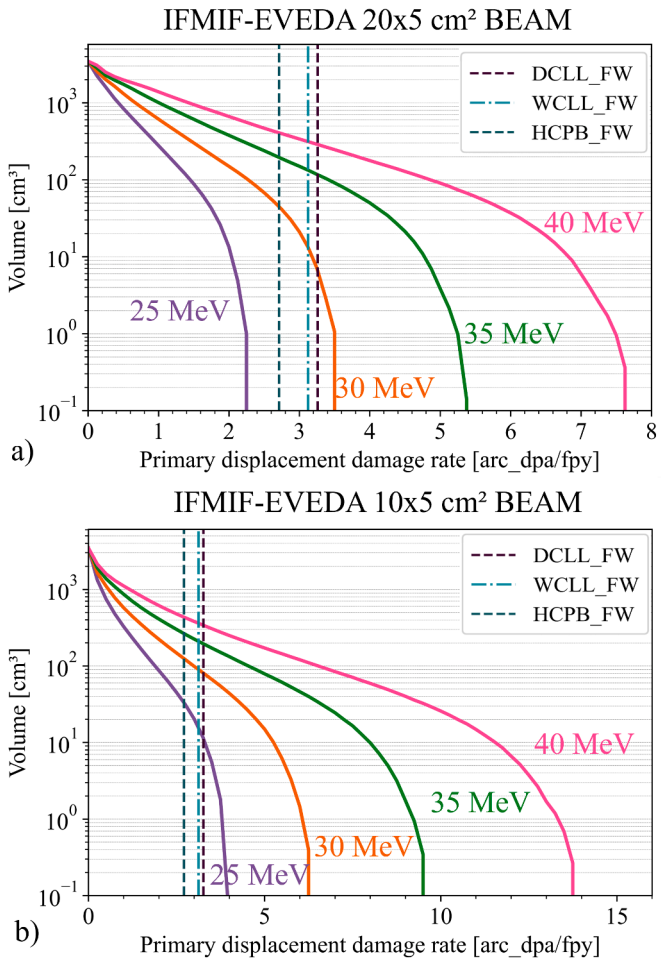

Fig. 19. Available integrated irradiation volume versus primary damage dose rate [arc_dpa/fpy] for the CLC.v2.0 model for 25, 30, 35, 45 MeV energy beam; a) 20×5 cm^2 and b) 10×5 cm^2 footprint size.

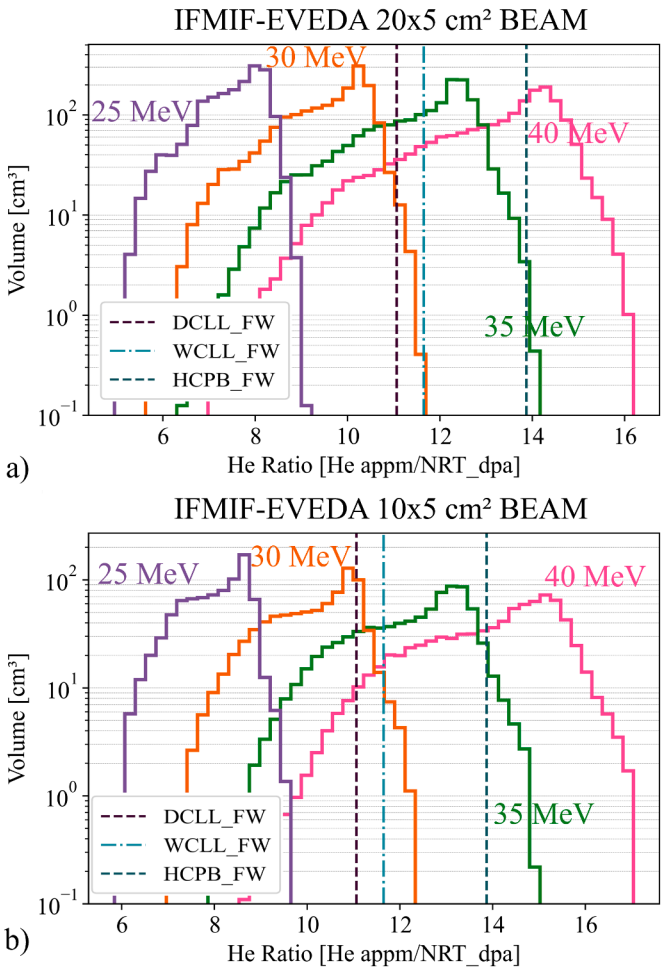

Fig. 20. Irradiation volumes as function of He-NRT_dpa ratio for the CLC.v2.0 model for 25, 30, 35, 45 MeV energy beam; a) 20×5 cm^2 and b) 10×5 cm^2 footprint size.

DEMO configurations, it is obtained that for all three cases, the value is around 3 arc_dpa/fpy. And as the tendency is the same as with NRT_dpa, IFMIF-DONES facility can reproduce the damage of 1 fpy of DEMO or more, depending on the beam energy. Moreover, the two beam footprints fulfil totally the DEMO requirements.

Figs. 20 and 21 show the He and H ratios calculated for different beam energies, for 20×5 cm^2 (panel a) and 10×5 cm^2 (panel b). As dpa values are lower when the energy beam decreases, the gas-DPA ratios follow this tendency. The gas-DPA ratios calculated for the DEMO designs considered are presented in each figure. The DEMO values are in a range of 11–14 He app/fpy and 45–55 H appm/fpy, which are consistent with the values presented in [28,29]. In the case of He rate using the standard beam (Fig. 20a) the energies of the IFMIF-DONES beam that fulfil the DEMO conditions are 35 and 40 MeV, while the other energies values reach lower values.. Meanwhile, using the reduced beam (Fig. 20b) the value of the energy beam that does not meet the conditions for any of the DEMO designs is 25 MeV. In the case of 30 MeV, the ratios for DCLL and WCLL are reached, but not for HCPB. Although using the higher energy beam values the He ratio reaches values of the order of DEMO requirements, the amount of available volume varies according to the energy. The values obtained for the H ratio present the same behaviour as the He one. The 35 and 40 MeV energy beams fulfil the DEMO conditions for the 20×5 cm^2 beam footprint (Fig. 21a) and in the case of the 10×5 cm^2 beam footprint (Fig. 21b), 30 MeV also meets the requirements, at least for some of the breeder concepts. So, in all the cases, the 35 MeV energy beam reaches adequate values for gas production, with the penalty of losing some high-DPA volume.

Considering the arc_dpa method for the primary displacement damage rate, the H gas production ratio expected for DEMO in the first wall is in the range of 168 – 200 [H appm/arc_dpa] and the calculated value for He gas production 40 – 50 [He appm/arc_dpa]. Fig. 22 and Fig. 23 show the gas production of H and He in the IFMIF-DONES facility for different beam energies and the data expected in DEMO. The tendency is the same with respect to the NRT_dpa calculations. The lowest energy of the beam 25 MeV does not reach the gas production expected in DEMO for any of the beam footprint sizes. Conclusions are very similar with comparisons based on NRT_dpa.

4. Conclusions

This study presents a radiation effects comparison of different distributions of the specimens inside the HFTM in IFMIF-DONES. Parameters such as neutron fluence rate, He and H production rates and primary displacement damage have been obtained for the different geometries. The new distribution of specimens in rigs, CLC.v2.0, has been compared with the CLC.v1.0 model and homogeneous one. CLC.v2.0 distribution increases the percentage of EUROFER97, reaching similar values of the homogeneous model, decreasing the amount of sodium, and increasing the number of specimens per rig. The beam profile used is IFMIF-EVEDA in two footprint beam sizes 20×5 cm^2 and 10×5 cm^2. The temperature in each rig has been also considered to understand the distribution of specimens as a function of primary displacement damage.

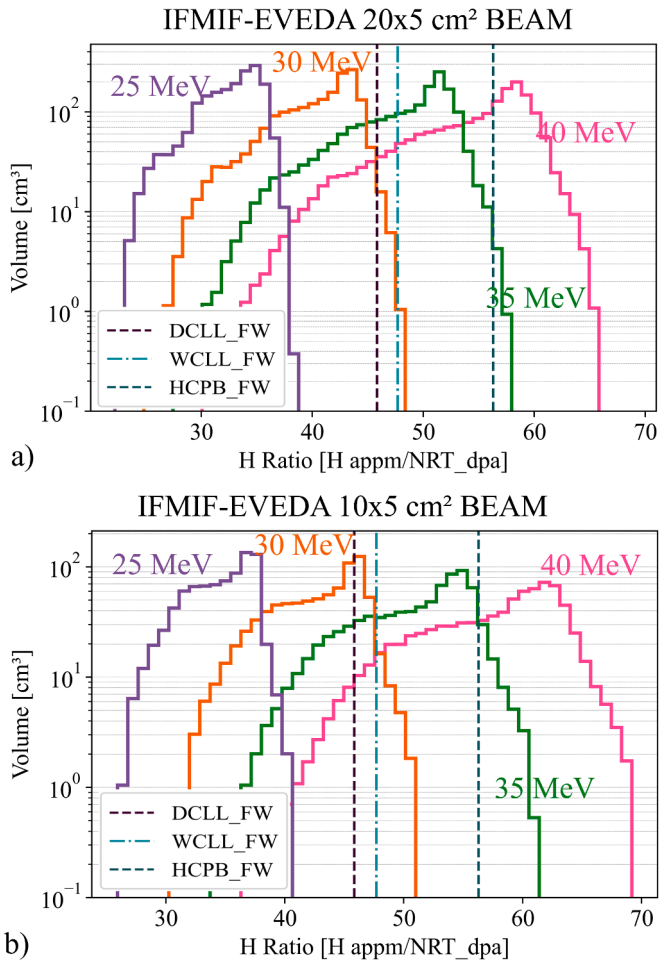

Fig. 21. Irradiation volumes as function of H-NRT_dpa ratio for the CLC.v2.0 model for 25, 30, 35, 45 MeV energy beam; a) 20×5 cm^2 and b) 10×5 cm^2 footprint size.

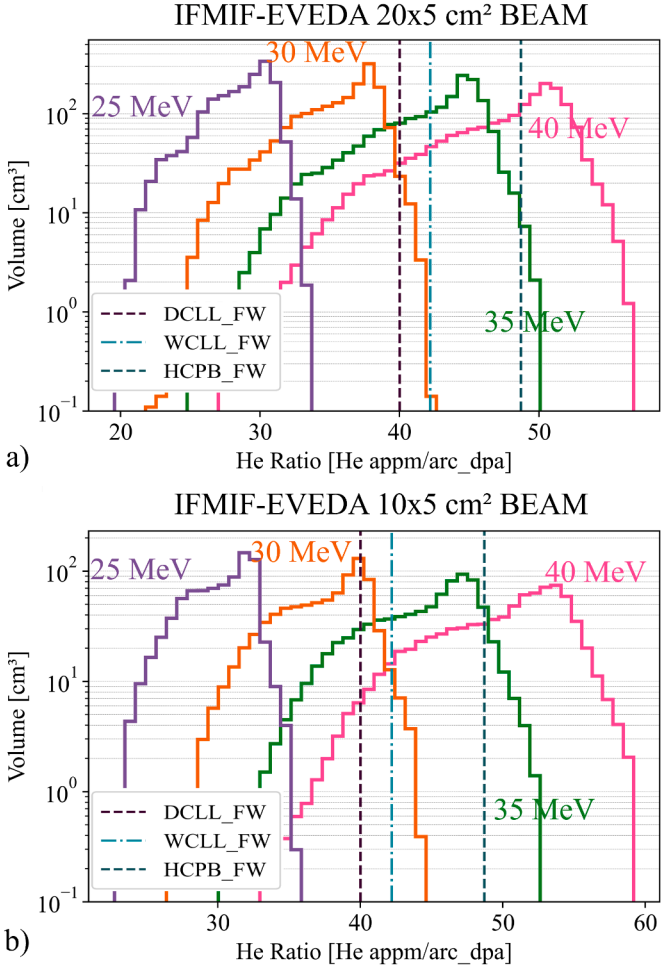

Fig. 22. Irradiation volumes as function of He-arc_dpa ratio for the CLC.v2.0 model for 25, 30, 35, 45 MeV energy beam; a) 20×5 cm^2 and b) 10×5 cm^2 footprint size.

Neutron fluence rate, primary displacement damage and gas production obtained with the CLC.v2.0 model and the homogenous one are very similar since the percentage of EUROFER97 and sodium in both models does not differ significantly. This is crucial because the approximations used in the homogeneous model are well-founded to represent the detailed model. Comparing the results of using CLC.v1.0 with CLC.v2.0 models, the primary displacement damage rate is lower in the first one due to the percentage of EUROFER97 is lower and higher the amount of sodium.

The distribution of specimens in the CLC.v2.0 allows to have all types in all the primary displacement damage ranges, whereas considering the CLC.v1.0 model, some specimen types disappear in the highest range of primary displacement damage. The temperatures previously established for each rig have been taken into account in this work. So, the primary displacement damage distribution versus specimen type and temperature have been calculated for the two beam footprints. Generally, using the 20×5 cm^2 footprint size, the number of specimens available in each dpa value range and temperature have a homogeneous tendency. On the other hand, the reduced beam footprint creates a heterogeneous distribution of dpa values by specimen type and temperature.

The influence of the deuteron beam energy on the results has also been analysed. Primary displacement damage rates, He and H ratios have been obtained for a beam of 25, 30, 35 and 40 MeV. These data have been compared directly to the data expected for the DCLL, WCLL and HCPB DEMO configurations, always considering the data from the inboard first wall. The values expected for DEMO are totally fulfilled by the IFMIF-DONES facility. Depending on the beam energy one or more fpy of DEMO operation can be reproduced for the primary displacement damage rates and the volume available for the He and H ratios is better fulfilled by the 35 MeV energy beam, although satisfactory results can be obtained with different volume distribution from energies of 30 to 40 MeV. It is also important to note that, the use of lower deuteron beam energy will reduce the high-DPA volume, thus the trade-off between them has to be deliberated.

CRediT authorship contribution statement

I. Álvarez: Writing – review & editing, Writing – original draft, Validation, Software, Methodology. **M. Anguiano:** Writing – review & editing, Writing – original draft, Validation, Supervision, Project administration, Methodology, Investigation, Funding acquisition. **F. Mota:** Writing – review & editing, Writing – original draft, Validation, Supervision, Software, Methodology, Funding acquisition, Conceptualization. **R. Hernández:** Writing – review & editing, Supervision, Resources. **F. Moro:** Writing – review & editing, Supervision, Resources. **S. Noce:** Writing – review & editing, Supervision, Resources. **Y. Qiu:** Writing – review & editing, Supervision, Resources. **J. Park:** Writing – review & editing, Supervision, Resources. **F. Arbeiter:** Writing – review & editing, Supervision, Resources. **I. Palermo:** Writing – review & editing, Supervision, Resources. **D. Sosa:** Writing – review & editing, Supervision, Resources.

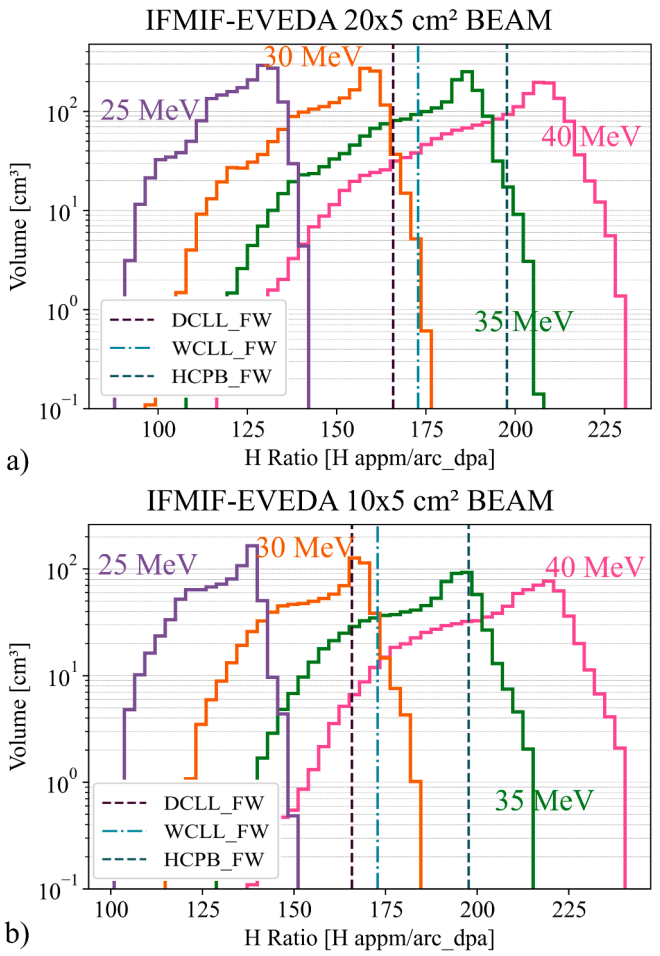

Fig. 23. Irradiation volumes as function of H-arc_dpa ratio for the CLC.v2.0 model for 25, 30, 35, 45 MeV energy beam; a) 20×5 cm^2 and b) 10×5 cm^2 footprint size.

Declaration of competing interest

The authors declare that they have no known competing financial interests or personal relationships that could have appeared to influence the work reported in this paper.

Acknowledgments

This work has been supported by the European Union's FEDER program, IFMIF-DONES Junta de Andalucia's program at the Universidad de Granada, by MCIN/AEI/10.13039/501100011033/FEDER, UE (PID2022–137543NB-I00) and has been carried out within the framework of the EUROfusion Consortium, funded by the European Union via the Euratom Research and Training Programme (Grant Agreement No 101052200 — EUROfusion). Views and opinions expressed are however those of the author(s) only and do not necessarily reflect those of the European Union or the European Commission. Neither the European Union nor the European Commission can be held responsible for them. This paper has been funding for open access charge: Universidad de Granada / CBUA.

Data availability

The authors do not have permission to share data.

References

[1] J. Knaster, A. Ibarra, J. Aba, A. Abou-Sena, F. Arbeiter, et al., The accomplishment of the engineering design activities of IFMIF/EVEDA: the European–Japanese project towards a Li(d,xn) fusion relevant neutron source, Nuclear Fusion 55 (2015) 086003 (30pp).
[2] A. Ibarra, R. Heidinge, P. Barabaschi, F. Mota, A. Mosnier, P. Cara, FS. Nitti, A stepped approach from IFMIF/eveda toward IFMIF, Fusion Sci. Technol. 66 (2014) 252–259.
[3] D. Bernardi, F. Arbeiter, M. Cappelli, U. Fischer, A. García, et al., Towards the EU fusion-oriented neutron source: the preliminary engineering design of IFMIF-DONES, Fusion Eng. Design 146 (2019) 261–268.
[4] Y. Qiu, M. Ansorge, I. Álvarez, K. Ambrožič, T. Berry, et al., Overview of recent advancements in IFMIF-DONES neutronics activities, Fusion Eng. Design 201 (2024) 114242, https://doi.org/10.1016/j.fusengdes.2024.114242. ISSN 0920-3796.
[5] G. Federici, et al., Overview of EU DEMO design and R&D activities, Fusion Eng. Des. 89 (2014) 882–889.
[6] A. Ibarra et al "White book on the complementary scientific programme at IFMIF-DONES" EFDA_D_2MP66K, https://idm.euro-fusion.org/?uid=2MP66K.
[7] G.R. Odette, P.J. Maziasz, J.A. Spitznagel, Fission– fusion correlations for swelling and microstructure in stainless steels: effect of the helium to displacement per atom ratio, J. Nucl. Mater. 103–4 (1981) 1289–1304.
[8] B. Van der Schaaf, et al., The development of EUROFER reduced activation steel, Fusion Eng. Design 69 (1–4) (2003) 197–203, https://doi.org/10.1016/S0920-3796(03)00337-5, n.
[9] Y. Qiu, F. Arbeiter, U. Fischer, F. Schwab, IFMIF-DONES HFTM neutronics modeling and nuclear response analyses, Nuclear Mater. Energy 15 (2018) 185–189, https://doi.org/10.1016/j.nme.2018.04.009.
[10] I. Álvarez, M. Anguiano, F. Mota, R. Hernández, Y. Qiu, Neutronic assessment of the IFMIF-DONES HFTM specimen stack distribution, Fusion Eng. Design 200 (2024) 114212, https://doi.org/10.1016/j.fusengdes.2024.114212. ISSN 0920-3796.
[11] F. Arbeiter "Summary of HFTM SRO activities and update of the Engineering design in 2023" (2023) EFDA_D_2RHEUV https://idm.euro-fusion.org/default.aspx?uid=2RHEUV.
[12] I. Fernández-Berceruelo, I. Palermo, F.R. Urgorri, A. García, D. Rapisarda, et al., Alternatives for upgrading the EU DCLL breeding blanket from MMS to SMS, Fusion Eng. Design 167 (2021), https://doi.org/10.1016/j.fusengdes.2021.112380.
[13] D. Rapisarda, I. Fernández-Berceruelo, A. García, J.M. García, B. Garcinuño, et al., The European Dual Coolant Lithium Lead breeding blanket for DEMO: status and perspectives, Nuclear Fusion 61 (2021), https://doi.org/10.1088/1741-4326/ac26a1.
[14] P. Arena, A. Del Nevo, F. Moro, S. Noce, R. Mozzillo, et al., The DEMO water-cooled lead–lithium breeding blanket: design status at the end of the pre-conceptual design phase, Appl. Sci. 11 (2021), https://doi.org/10.3390/app112411592.
[15] F. Moro, P. Arena, I. Catanzaro, A. Colangeli, A. Del Nevo, et al., Nuclear performances of the water-cooled lithium lead DEMO reactor: Neutronic analysis on a fully heterogeneous model, Fusion Eng. Design 168 (2021) 112514, https://doi.org/10.1016/j.fusengdes.2021.112514. ISSN 0920-3796.
[16] I. Palermo, F.A. Hernández, P. Pereslavtsev, D. Rapisarda, G. Zhou, Shielding design optimization of the helium-cooled pebble bed breeding blanket for the EU DEMO fusion reactor, Energies. (Basel) 15 (2022), https://doi.org/10.3390/en15155734.
[17] G. Zhou, F.A. Hernández, P. Pereslavtsev, B. Kiss, A. Retheesh, et al., The European DEMO helium cooled pebble bed breeding blanket: design status at the conclusion of the pre-concept design phase, Energies. (Basel) 16 (2023), https://doi.org/10.3390/en16145377.
[18] G. Zhou, J. Aktaa, D. Alonso, L.V. Boccaccini, I. Cristescu, et al., "Design update of the European DEMO helium cooled pebble bed breeding blanket" (CBBI-21 2023), Granada, Spanien, 19.–20. Oktober 2023. https://publikationen.bibliothek.kit.edu/1000165661.
[19] SpaceClaim 3D software, url: https://www.ansys.com/products/3d-design/ansys-spaceclaim.
[20] C.J. Werner et al 2018 MCNP version 6.2 release notes (LA-UR-18-20808) (Los Alamos National Laboratory) (https://laws.lanl.gov/vhosts/mcnp.lanl.gov/pdf_files/la-ur-18-20808.pdf).
[21] Y. Wu, Multi-functional neutronics calculation methodology and program for nuclear design and radiation safety evaluation, Fusion Sci. Technol. 74 (2018) 321–329.
[22] A. Konobeyev, Yu. Korovin, P. Pereslavtsev, U. Fischer, U. Von Mollendorff, Development of methods for calculation of deuteron-lithium and neutron-lithium cross sections for energies up to 50 MeV, Nucl. Sci. Eng. 139 (2001) 1–23.
[23] FENDL-3.1d: fusion evaluated nuclear data library Ver.3.1d, https://www-nds.iaea.org/fendl/.
[24] M.J. Norgett, M.T. Robinson, I.M. Torrens, A proposed method of calculating displacement dose rates, Nucl. Eng. Des. 33 (1975) 50–54, https://doi.org/10.1016/0029-5493(75)90035-7.
[25] K. Nordlund, S.J. Zinkle, A.E. Sand, F. Granberg, R.S. Averback, et al., Improving atomic displacement and replacement calculations with physically realistic damage models, Nat. Commun. 9 (2018) 1084, https://doi.org/10.1038/s41467-018-03415-5.
[26] JEFF3.3DPAarc, https://www.oecd-nea.org/dbdata/jeff/jeff33/index.html.

[27] F. Schwab, S. Gordeev, Y. Qiu and A. Abou-Sena "High flux test module (250-550°C RAFM irradiation)" technical note EFDA_D_2MUEU3 (2018).
[28] D. Stork, P. Agostini, J.-L. Boutard, et al., Materials R&D for a timely DEMO: key findings and recommendations of the EU roadmap materials assessment group, Fusion Eng. Des. 89 (2014) 1586–1594.
[29] M.R. Gilbert, S.L. Dudarev, S. Zheng, L.W. Packer, J.C. Sublet, An integrated model for materials in a fusion power plant: transmutation, gas production, and helium embrittlement under neutron irradiation, Nucl. Fusion 52 (2012) 083019, https://doi.org/10.1088/0029-5515/52/8/083019.